Biochimica et Biophysica Acta, 466 (1977) 68—83

BBA 77650

POLYOL PERMEABILITY OF THE HUMAN RED CELL

INTERPRETATION OF GLUCOSE TRANSPORT IN TERMS OF A PORE

ROBERT J. BOWMAN [a] and DAVID G. LEVITT [b]

[a] *Department of Laboratory Medicine and Pathology, University of Minnesota Medical School, Minneapolis, Minn. 55455 and St. Paul Regional Red Cross Blood Center, St. Paul, Minn. and* [b] *Department of Physiology, University of Minnesota Medical School, Minneapolis, Minn. 55455 (U.S.A.)*

(Received October 28th, 1976)

Summary

The kinetic equations describing transport through a pore that has a binding site and that undergoes a conformational change are identical to those of a carrier model. Therefore, in order to distinguish between the two models it is necessary to test specific predictions based on detailed mechanistic models. A pore model is described in which the substrate (glucose) is able to reach the single binding site only from the outside when the pore is in conformation I and only from the inside when it is conformation II. On the basis of this model it is predicted that solutes which do not have any specific affinity for the binding site should still have a finite permeability via the glucose transport system if they are the same size or smaller than glucose. This permeability should be proportional to the volume of distribution of the solute in the pore and should therefore decrease with increasing molecular size. A geometric pore volume can be estimated from this size dependence. In order to test these predictions, the glucose-dependent permeability of a series of 4-carbon (erythritol), 5-carbon (D-arabitol, L-arabitol and xylitol) and 6-carbon (D-mannitol, D-sorbitol and *myo*-inositol) polyols was measured. The permeability of all the polyols is decreased by the presence of glucose and the K_I of this "inhibitable" component is similar to that of D-sorbose, suggesting that this component is associated with the glucose transport system. Since these observations could be explained entirely in terms of a specific affinity for a carrier binding site, they do not exclude a carrier mechanism. However, as predicted for the pore model, this "inhibitable" permeability decreased with increasing molecular size and the calculated geometric pore volume was of a size that would be expected for a cell membrane pore.

Introduction

Recent experiments have shown that the kinetics of glucose transport in the human red blood cell cannot be satisfactorily described by a symmetrical carrier model. Geck [1] and Regen and Tarpley [2] have shown that a generalized version of this model (in which no assumptions are made about symmetry or the relative rate of binding versus transport of the carrier) can account for most of the experimental measurements. However, as has been pointed out by Britton [3], a carrier mechanism is not a unique physical realization of the kinetic equations of the general carrier model since exactly the same set of equations describe a pore model that undergoes a conformational change. In a recent review, Singer [4] has concluded from a general analysis of membrane properties that pores are probably involved in facilitated transport systems.

The details of the pore model are, of course, not unique and a number of variations can be imagined. We chose the model in Fig. 1 in order to provide a simple and specific example of a "prototype" pore. The pore contains a single substrate (glucose) binding site and can exist in two conformational states: State I, in which the substrate can reach the binding site only from the outside; and State II, in which the substrate can reach the binding site only from the inside. The meaning of the various rate constants is indicated in the figure legend. For example, the constants k_4 and k_{-4} are a measure of either the rate of movement of the unbound carrier in the two directions or of the rate of conformational change of a pore that does not contain a substrate molecule.

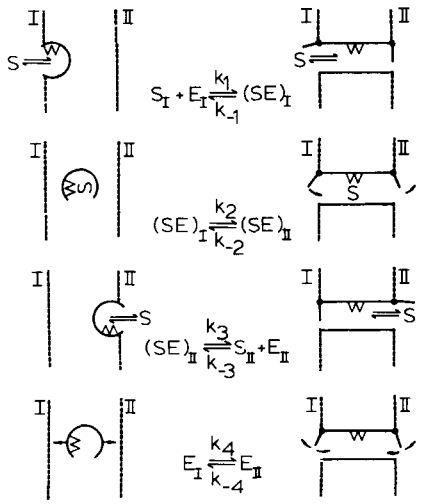

Fig. 1. Comparison of the kinetic description of a carrier (left) and a pore model (right). Both models have a single binding site for substrate (S). The rate constants k_1 and k_{-1} refer to association and dissociation of substrate, respectively, with the binding site when carrier is located on side I or when the pore is open to side I. The constants k_3 and k_{-3} have the same meaning on side II. The rate constants k_2 and k_{-2} refer either to translocation of carrier or to the conformational change (schematically indicated by swinging gates) when substrate is bound to the binding site. Similarly k_4 and k_{-4} refer to carrier translocation or to the conformational change in the absence of bound substrate. Both models are described by exactly the same kinetic equations.

Authors in several recent studies [5–7] have in fact chosen such a pore model as the most reasonable one for interpreting their biochemical investigations of the glucose transport system. A major reason for this choice is that a pore model requires only a slight modification of well established enzyme mechanisms. Since enzymes also have a binding site and undergo conformational changes, all that is needed is to place the binding site in a pore that spans the membrane. The required conformational changes (represented by the swinging of the gates in Fig. 1) are not large. A 1 or 2 Å movement of a group at one end of a pore is enough to change a pore from an open to closed form with respect to glucose. In comparison, the carrier mechanism requires either rotational or translational movements of a large carrier molecule over distances of 10 Å or more. The pore model also provides a natural explanation of the asymmetry that is such a characteristic feature of the glucose transport system since one would expect that the affinity of the binding site and the rate of change from one state to the other should be different for the two states. In its simplest version, the carrier should have the same affinity on the two sides and the same rate of movement in the two directions.

Although it is impossible to distinguish between the two types of models on the basis of kinetic experiments, it should be possible to accumulate suggestive evidence that favors one of the models by testing various mechanistic predictions. For example, the observation that the presence of glucose alters the rate of inactivation of the glucose transport system by 1-fluoro-2,4-dinitrobenzene suggests that the system undergoes a conformational change at a rate that is altered by the presence of glucose, a result that is consistent with the pore model [5]. Additional support for the pore model comes from the investigation by Barnett et al. [6] of the asymmetrical affinity of a series of glucose analogues that could not, themselves, pass through the glucose transport system. In the interpretation of these results, the authors postulated that there was a single fixed site in a pore (as in Fig. 1) and that the asymmetry could be accounted for by the fact that the analogues were forced to approach the site from the two ends of the pore with different orientations.

The purpose of this paper is to quantitatively test the pore model for consistency with new data on the permeability of polyols. Although the experimental results will be shown to be consistent with the pore model, they may also be interpreted in terms of a carrier model, and, therefore, do not permit a definite distinction to be made between the two models. Our test is based on the idea that even if a solute did not have any specific affinity for the binding site, it would still have a finite permeability via this transport system. For example, for the pore model, a solute with no affinity for the binding site would still have a finite probability of being in the pore region between the gates and would be transported across the membrane by a conformational change. The probability of being in the pore should be directly related to the volume of distribution of the solute in the pore and should show a strong size dependence, decreasing to zero for molecules with a radius larger than the pore radius. One can apply the same kind of argument to the carrier model where now the "non-specific" permeability can be related to the volume of distribution at the carrier site. One would expect this volume to be much smaller than that of the pore model. Thus our test is based on measuring the permeability via the glucose transport system of

a series of solutes of varying size that we hoped would not have any specific affinity for the binding site. If a pore-like mechanism exists, this permeability should decrease with increasing molecular size and the quantitative volume of distribution of the solutes should be compatible with the dimensions expected for a membrane pore.

The observation [8—10] that a significant fraction of the red cell erythritol permeability is inhibited by glucose is strong evidence that this fraction is using the glucose transport system. This observation suggested to us the possibility of testing whether the glucose inhibitable permeability of a series of polyols is inversely proportional to their size. If the pore model is correct and if these molecules do not have any specific affinity for the binding site, then this component of the permeability of the 4-carbon polyol should be greater than that of the 5-carbon polyols which in turn should be more permeable than the 6-carbon polyols. As will be shown below, this size dependence is, in fact, observed for the human red cell. The question then arises as to whether this size dependence could also be explained by a carrier mechanism for which the permeability should depend on the relative affinity of the polyol for the binding site. This affinity should depend primarily on the stereochemical structure of the polyol and one might observe for example that a 6-carbon molecule of appropriate structure (i.e. sorbitol) has a higher permeability than a 5-carbon or 4-carbon compound. This question is considered in more detail in Discussion.

Methods

All of the results reported in this paper are from experiments on freshly drawn blood from one of us. The heparinized blood was washed twice with phosphate-buffered saline and then incubated in phosphate-buffered saline containing concentrations of glucose varying from 0 to 200 mM in order to equilibrate the cells with the desired glucose concentration. The incubation was performed at 39° C for 90 min with two washings. As determined by changes in cell volume measured by the microhematocrit method (see below) this period was sufficient to produce at least 90% equilibration of the cells in 200 mM glucose. All the experiments were performed at 39° C. The buffered saline was made by mixing three parts 0.1 M sodium phosphate (titrated to pH 7 with 1 M HCL) with seven parts 0.9% NaCl. No significant difference was noted in one experiment in which calcium (2.15 mM) was added. The ^{14}C-labeled compounds were obtained from New England Nuclear (D-mannitol, sucrose, D-sorbitol, D-glucose), Calatomic (L-arabitol) and Amersham/Searle (erythritol) and the *myo*-[^{3}H]-inositol was obtained from New England Nuclear.

Permeability measurements from tracer uptake

Packed cells (0.5 ml) equilibrated at the desired glucose concentration were mixed with 1.5 ml of phosphate-buffered saline at the same glucose concentration and with about 1.0 μCi of the labeled solute and varying amounts (usually about 5 mM) of unlabeled solute. At varying time intervals, 0.2 ml of the cell suspension was sampled and immediately injected into 10 ml of 1.8% unlabeled ice-cold saline. The cells were centrifuged at 5° C, the supernatant removed, and

the cells again suspended in 10 ml of cold saline, centrifuged and the supernatant removed. The cell button (about 0.05 ml) was dispersed with a stirring rod and 0.3 ml of Protosol (New England Nuclear) was added to solubilize the cells. The solution was stirred for 3 min and then 0.3 ml of a saturated solution of benzoyl peroxide in toluene was added to bleach the hemoglobin. The mixture was transferred quantitatively to a scintillation vial by washing the centrifuge tube with Aquasol (New England Nuclear). The vials were counted in a Packard scintillation counter. The ^{14}C counting efficiency for samples treated this way was about 95% of that for a control sample without any cells. The initial extracellular label was determined by treating 0.1 ml of the total cell suspension in the same manner.

The effectiveness of the washing procedure was determined by injecting the cell suspension into the cold saline at $t = 0$ and assuming that all the counts represented trapped extracellular solute. This procedure indicated that the trapped volume was relatively constant and was equivalent to about 0.5% of the cell volume. The effectiveness of 1.8% ice-cold saline "stopper" solution was tested by measuring the changes in washed cell isotope concentration as a function of time in the stopper. No significant changes were noted for periods of up to 2 h.

The membrane permeability (P) was determined from the following equation (see Appendix)

$$\ln(1 - A_c/A_c^{eq}) = -\lambda P' t \tag{1}$$

$$\lambda = \frac{1 - H(1 - K)}{1 - H}, \qquad A_c^{eq} = \frac{KHA_T}{1 - H(1 - K)}, \qquad P' = \frac{PS}{v_{cw}}$$

where A_c and A_c^{eq} are the amount of radioactivity in the washed cells from a unit volume of incubation medium at time t and at equilibrium, respectively; A_T is the total radioactivity in a unit volume of incubation medium; H is the hematocrit; and K is the water fraction of the cells. We used a value of $155 \cdot 10^{-8}$ cm^2 for the surface area of the cell (S) and a value of $63 \cdot 10^{-12}$ cm^3 for the cell water volume (v_{cw}) [11]. A value for K of 0.65 was determined from the equilibrium volume of distribution (at 2 h) of the labeled erythritol. A plot of the left side of Eqn. 1 versus t should be a straight line and the permeability (P) can be determined from the slope.

Permeability measurements from changes in cell volume

In order to provide an independent check of the isotope procedure and to determine the permeability of solutes that were not commercially available with a radioactive label, we developed a method for determining the permeability from the change in cell volume resulting from the permeant entering the cell.

Washed cells were equilibrated in phosphate-buffered saline with glucose (0 and 50 mM) for 90 min with two washes. Equilibrated cells were then centrifuged (hematocrit about 70%) and added to a solution of permeant adjusted so that the final concentration of permeant was 150 mM with glucose and phosphate buffer concentrations unchanged. The change in cell volume was deter-

mined by sampling the cell suspension and spinning in a microhematocrit centrifuge for 5 min. The time between sampling and starting the centrifuge was 1—2 min which was negligible relative to the half time of cell swelling. The permeability was determined by numerically generating theoretical volume curves for different values of P (see Appendix) and then choosing the value of P that best fit the experimental data.

Cell suspensions that contain glucose in addition to permeant solute introduce an additional complication since, as the cell swells, the intracellular glucose concentration will change and it must be shown that the rate of equilibration of the glucose is fast relative to movement of the test solute if the swelling rate is to be used as a measure of the test solute permeability. Using the equations of Regen and Tarpley [2] and extrapolating their rate constants to 39°C it can be shown that at a glucose concentration of approx. 50 mM inside and outside the cell the half time of glucose equilibration is about 2 min, which is fast relative to the half times of the test solute movement (about 50 min). However, the half time for glucose becomes about 30 min at concentrations of 200 mM, and this is slow enough to affect the results. For this reason, the maximum glucose concentration used in these experiments was 50 mM. Sucrose was used as an impermeant control in order to show that all the volume change was due to the movement of the test solute.

Effect of tracer impurities

The uptake of mannitol and sucrose (not corrected for trapped volume) as a function of time for impure ^{14}C label is shown in Fig. 2. It can be seen that in the absence of glucose the uptake extrapolates back to a point representing about 8% equilibration at $t = 0$ while in the presence of glucose, the curves extrapolate back to a significantly smaller value. It seemed unlikely that there could be as much as 8% impurity in the label because several different batches of labeled mannitol from different companies gave similar results. When the sucrose was chromatographed on a Sephadex G-10 column and label from the front of the elution profile was retested the points now extrapolated back to a value of 0.7% equilibrium which is approximately equal to the trapped volume (Fig. 3). Since the elution profile from the Sephadex G-10 column did not show an impurity of the magnitude expected, it occurred to us that if there was a 1—2% glucose (or other metabolite) impurity, then its ^{14}C could become distributed in the entire carbon pool of the glycolytic pathway and, in the absence of glucose (or other carbon compound) in the external medium, label might become concentrated in the cells. Since the hematocrit was about 17% in these experiments there could have been an 8-fold concentration if all the impurity was concentrated in the cells. To test this idea we repeated the experiments with a 2% hematocrit and found, as predicted, that the points now extrapolated back to a much larger value (30%) at $t = 0$. We also incubated the cells in trace amounts of [^{14}C]glucose and found, as expected, that the ^{14}C was concentrated about 6-fold in the cells at a hematocrit of 16%. This explanation also provided us with a simple means of purifying the mannitol label. When labeled mannitol was incubated in the absence of glucose for 2 h with a 50% hematocrit, the impurity was concentrated by the cells and completely removed from the supernatant. When the uptake of this purified mannitol was measured

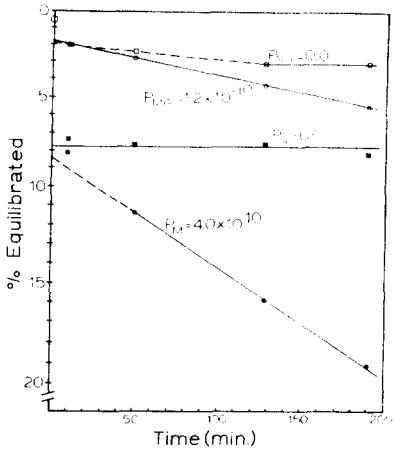

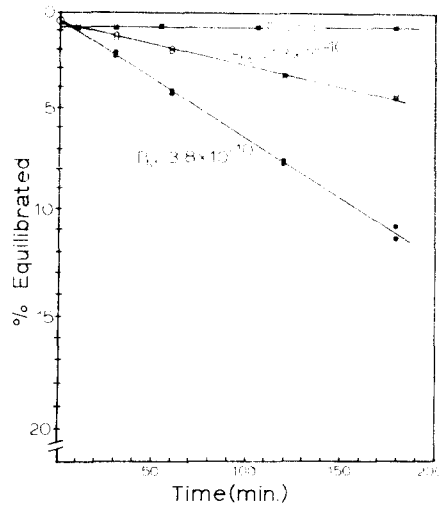

Fig. 2. A semilog plot of the percent uptake of the unpurified ^{14}C-labeled mannitol in zero (•) or 200 mM (○) glucose and of unpurified ^{14}C-labeled sucrose in zero (■) or 200 mM (□) glucose. The numbers indicate the permeabilities (cm/s) for the indicated solid straight lines. The uptake is not corrected for the trapped volume which is indicated by the circle at $t = 0$.

Fig. 3. Same plot as in Fig. 2, but for the purified [^{14}C]mannitol (two different experiments) in zero (•) or 200 mM (○) glucose and sucrose in zero (■) glucose.

(Fig. 3) the points now extrapolated back to 0.5% (the trapped volume). All the results reported in this paper are for labeled mannitol and sorbitol purified by this procedure. This artifact can be even more confusing when the incubations are carried out in solutions that have initially low glucose concentration. As the glucose in the medium becomes exhausted the cells begin to concentrate the labeled impurity and one observes a very misleading time course of ^{14}C uptake. The criteria of purity that we applied in this paper was that all the points must be satisfactorily fitted by a single exponential that extrapolated back to about 0.5% (the trapped volume). In addition, the permeability measurements for L-arabitol and D-mannitol were confirmed by measurements based on changes in cell volume, a procedure which did not require the use of radioactive labels.

Results

Permeabilities from tracer uptake

The permeabilities of erythritol, L-arabitol, D-mannitol, D-sorbitol and *myo*-inositol in the presence of 0 and 200 mM glucose are listed in Table I. The permeabilities were independent of solute concentration in the range of 0—50 mM. If erythritol, L-arabitol and D-mannitol were all using the same transport system, then their permeability (P_i) should be described by the following equation (where G is the glucose concentration):

$$P_i(G) = \frac{P_i^I}{1 + G/B} + P_i^N \qquad (2)$$

TABLE I

PERMEABILITY (10^{-10} cm/s) FROM ISOTOPE UPTAKE

Results are given as the mean ± S.E. and the number of experiments is in parentheses

	$G = 0$	$G = 200$ mM	10^{-4} M phoretin	P^I	P^N
Erythritol	908 ± 26 (4)	360 ± 9 (4)	336 (1)	569	338
L-Arabitol	46.1 ± 1.8 (4)	22.3 ± 2.1 (4)	25 (1)	25	21
D-Mannitol	3.71 ± 0.15 (4)	1.19 ± 0.08 (4)	1.2 (1)	2.62	1.09
D-Sorbitol	4.03 ± 0.08 (3)	2.78 ± 0.07 (3)		1.30	2.73
myo-Inositol	17.56 ± 0.62 (4)	0.89 ± 0.09 (3)		6.94	0.62

The form of the first term, which represents the glucose inhibitable component, comes directly from the assumption that the transport system obeys the general kinetic equations shown in Fig. 1 [2]. The subscript i refers to the specific solute. If the three solutes are using the same transport system, then the inhibition constant B, which is a measure of the affinity of the system for glucose, should be the same for all three, although they would have different maximum inhibitable (P_i^I) and non-inhibitable (P_i^N) permeabilities. From Eqn. 2, one can define the function F_I which is a measure of the fractional degree of inhibition by glucose and should be independent of the solute studied:

$$F_I = \frac{P_i(0) - P_i(G)}{P_i(0) - P_i(200)} = G(B^{-1} + 200^{-1})/(1 + G/B) \qquad (3)$$

Fig. 4 shows F_I as a function of glucose concentration for the three solutes. It can be seen that all three solutes have the same functional dependence on the glucose concentration, consistent with the idea that they are all using the same transport system. In addition, the experimental points can be fitted fairly well by Eqn. 3 (solid line) with B equal to 8 mM. This value of B is close to the value of 10 mM found for the glucose inhibition of D-sorbose transport [12]. Since it is generally accepted that D-sorbose is using the glucose transport system, we feel that this similarity is strong evidence that the polyols are also using this system. By using this value of B in Eqn. 2, the values of the inhibitable (P_i^I) and non-inhibitable (P_i^N) permeabilities can be determined for the

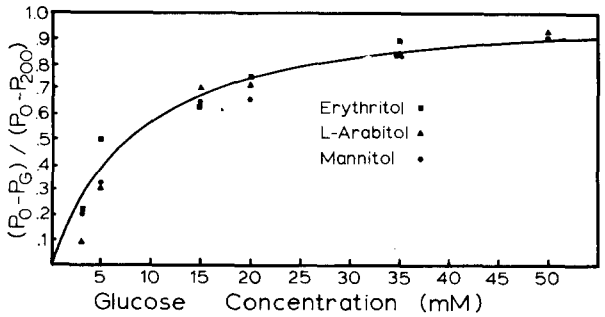

Fig. 4. Relative inhibition of the glucose-inhibitable permeability of erythritol, L-arabitol and D-mannitol as a function of glucose concentration. The solid line is the theoretical curve for an inhibition constant of 8 mM.

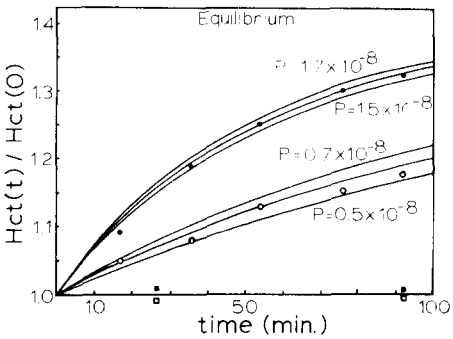

Fig. 5. Change in red cell hematocrit (Hct (t)) relative to initial hematocrit (Hct (0)) as a function of time for D-arabitol in zero (●) and 50 mM (○) glucose and sucrose in zero (■) and 50 mM (□) glucose. The solid lines are the theoretical curves for the indicated permeabilities (cm/s). The solid line at the top of the graph represents the relative hematocrit at equilibrium.

individual solutes (Table I). The effect of phloretin on the permeability of the three solutes was also tested and there was no significant difference between the effects of 200 mM glucose and 10^{-4} M phloretin. This is further evidence that the three solutes were all using the glucose transport system.

Permeabilities from volume measurements

Fig. 5 shows the change in hematocrit as a function of time for D-arabitol and sucrose in 0 and 50 mM glucose. The solid lines are the theoretical curves for different values of P. It can be seen that the change in cell volume is satisfactorily described by the theory. There were no significant volume changes in sucrose for at least 5 h. Table II lists the permeabilities in 0 and 50 mM glucose of D- and L-arabitol and xylitol. Using these values and the value of B of 8 mM determined from the tracer experiments, the value of the glucose inhibitable (P_i^I) and non-inhibitable (P_i^N) permeabilities can be determined from Eqn. 2 (Table II). The values for L-arabitol are slightly lower than those determined by the tracer method (Table I) and are probably less reliable because of the error inherent in the hematocrit measurements. The permeability of D-mannitol was also measured by this method, but in only one experiment. Because of the very small permeability of mannitol, the hematocrit measurements were subject to considerable error even when a time period of 5 h was used. In any case, the permeability values of $3 \cdot 10^{-10}$ ($G = 0$) and $1.5 \cdot 10^{-10}$ ($G = 200$ mM) were approximately the same as were found by the tracer method and provide an independent check of that method.

TABLE II

PERMEABILITY (10^{-10} cm/s) FROM RATE OF CELL SWELLING

Results are given as the mean ± S.E. and the number of experiments is in parentheses

	$G = 0$	$G = 50$ mM	P^I	P^N
L-Arabitol	41 ± 5 (6)	18 ± 2 (5)	27	14
D-Arabitol	124 ± 13 (5)	40 ± 7 (4)	97	26
Xylitol	75 ± 10 (4)	45 ± 3 (3)	35	40

Discussion

Our permeability values for erythritol confirm the previous results of Wieth [9] and LaCelle and Passow [10]. By following changes in cell volume measured by light scattering, Faust [13] found that for both D- and L-arabitol the half time was 29 min (which corresponds to a permeability of about $2.3 \cdot 10^{-8}$ cm/s at 37° C, pH 7) in the absence of glucose and the isomers were not significantly different. He did not measure the glucose-inhibitable permeability. Within the resolution of his apparatus, D-mannitol and D-sorbitol appeared to be impermeable. This indicates that his measurements were not sufficiently sensitive for the slowly permeable solutes and probably explains why he did not observe the difference between L- and D-arabitol that we found and why his values are significantly larger than ours (Table I). Although it is usually assumed that D-mannitol and *myo*-inositol are impermeants for the red blood cells, this assumption is based on relatively short term swelling experiments [14,15] that probably would not have detected the small permeability found in our experiments.

Glucose-inhibitable permeability

The glucose-inhibitable permeabilities are shown in Tables I and II. The dependence on size is obvious and is just what would be predicted for the pore model. That is, the inhibitable permeability of the 4-carbon compound is greater than for all the 5-carbon compounds which are greater than for all the 6-carbon compounds. Although there is no overlap between polyols of different size, there is considerable variability within each size group. For example, among the 5-carbon compounds, D-arabitol is about three times more permeable than L-arabitol and xylitol. Similarly, for the 6-carbon compounds, *myo*-inositol is significantly more permeable than D-mannitol and D-sorbitol. This variability is expected since the volume of distribution in the pore should depend on more than just the number of carbon atoms in the polyol. There may be small differences in the affinity for the glucose binding site or in the ability to form hydrogen bonds with the pore wall. Both of these factors would lead to differences in the partition of the polyols between the aqueous medium and the pore and would depend on the stereochemical structure. In addition, not all of the polyols with the same number of carbon atoms have the same shape. For example, it has been recently shown that arabitol and mannitol have a straight chain conformation in chloroform while xylitol and sorbitol are in a bent or sickle conformation [16].

It is also possible to obtain a quantitative estimate of the geometric pore volume. This calculation provides a more stringent test of the pore model since the calculated pore volume must be compatible with a pore that spans a cell membrane (about 50 Å long) and that is slightly larger in radius than glucose (about 3.6 Å). The rate of transport (J) through the pore is equal to the probability of being in the pore times the turnover rate of the pore between the two states. If, as a first approximation, it is assumed that the conformational change is the rate-limiting step, then the probability of a "non-specific" molecule being in a pore is simply equal to the volume of distribution (v_p) times the concentration in the medium that the pore is open to. The turnover rate may be simply

related to the maximum glucose transport rate (which depends on the specific experimental conditions). This assumes that when glucose transport is occurring at a maximal rate, a molecule of glucose is transported each time the pore turns over. Thus,

$$J = v_p(C_1 - C_2)V_{max} = P(C_1 - C_2) \tag{4}$$

where V_{max} is given in molecules per unit time, per unit area of membrane. Solving Eqn. 4 for v_p:

$$v_p = \frac{P}{V_{max}} \tag{5}$$

It should be emphasized that v_p is the volume of distribution of the molecule, and is not the geometric volume of the pore. For example, if the distribution of the solute was ideally "non-specific" and all the restriction to entry was steric, then v_p would be equal to the volume available to the center of the molecule:

$$v_p = \pi(R - a)^2(L - b) \tag{6}$$

where R and L are the radius and length of the pore and a and b are the radius and length of the (assumed) cylindrical solute molecule.

The volume of distribution in the pore (v_p) determined by applying Eqn. 5 to the inhibitable permeabilities (P^I) is listed in Table III (column 3). Polyols which had a significantly higher P^I than other polyols of the same size were not included in Table III since, as was discussed above, they may have some affinity for the binding site. Since this permeability is a measure of the rate of conformational change in the absence of glucose, the V_{max} for "free carrier exchange" (which is approximately equal to the V_{max} for influx [2]) should be used in Eqn. 5. We choose $V_{max} = 5.87 \cdot 10^{13}$ molecules/s per cm^2 cell surface which was obtained by multiplying the value of V_{max} for glucose entrance obtained by Lacko et al. [17] at 20°C by a factor of 4, and using the values for cell surface area and volume given in Methods to adjust the units. The value of v_p calculated from the erythritol permeability (970 Å^3) is so large that it could not possibly represent a real pore volume and indicates (if the pore model is correct) that erythritol has some specific affinity for the binding site. However, the values of v_p for L-arabitol, xylitol, D-mannitol and D-sorbitol are in a range that is consistent with the pore model. As was emphasized above, v_p is not itself the volume of the pore and it should be a function of size of the molecule. For example, it can be shown for the idealized case described by Eqn. 6 that the

TABLE III

INHIBITABLE (v_p^I) AND NON-INHIBITABLE (v_p^N) PORE VOLUMES OF DISTRIBUTION

	P^I (10^{-10} cm/s)	v_p^I (Å^3)	P^N (10^{-10} cm/s)	v_p^N (Å^3)
Erythritol	569	970	338	98
L-Arabitol	25	43	21	6.1
Xylitol	35	59	40	12
D-Mannitol	2.62	4.5	1.09	0.32
D-Sorbitol	1.3	2.2	2.73	0.80

values of v_p for L-arabitol and D-mannitol correspond approximately to a pore that has a radius of 4 Å and a length of 23 Å (using the not unreasonable values of a = 3.0 Å, b = 10 Å for arabitol and a = 3.6 Å, b = 11 Å for mannitol). Although this calculation is highly oversimplified, it does show that the observed permeabilities are in rough quantitative agreement with the predictions of the pore model.

There is another, completely different, approach to interpreting this permeability data that is just as consistent with the pore model. It is possible that the pore is open at both ends simultaneously for a short time during the conformational change. The observed premeability would then be a measure of the flux through the pore during this short period. The relative inhibitable permeabilities of erythitol, arabitol and mannitol are approximately what would be predicted for a pore that would just allow glucose to pass [19].

Since the observed permeabilities could be explained entirely in terms of a specific affinity for a carrier binding site, these observations do not exclude a carrier mechanism. The strength of our argument that this data is evidence for a pore mechanism depends on what is regarded as the probability that the carrier affinity would have the strict size dependence that was observed. One might expect that the affinity for the polyols would increase (not decrease, as is observed) as the size of the polyol increased since the larger polyols should have a structure closer to that of glucose. On the other hand, it is possible that the smaller polyols are able to obtain a better fit at the binding site because they are able to take up a larger number of orientations. Based on this data, we believe that the strongest argument against a carrier is that all of the 5-carbon polyols had permeabilities larger than all of the 6-carbon polyols. There is enough variation in the stereochemical structure of these two sets of polyols that we would have expected the permeability of one or more of the 6-carbon polyols to exceed or at least approach that of the 5-carbon polyols if their permeability was determined entirely by affinity for the binding site.

Non-inhibitable permeability

Both Wieth [9] and LaCelle and Passow [10] considered various alternative explanations of the component of the erythritol permeability remaining in the presence of high glucose concentrations (non-inhibitable) and concluded that it represented a completely independent pathway, probably dissolution and diffusion through the lipid part of the membrane. The non-inhibitable permeabilities (Tables I and II) are similar to the values that have been found for pure lipid membranes. For example, for bilayer membranes made from lipid extracts of human red cells, Jung [20] obtained a permeability of $2.3 \cdot 10^{-10}$ and $0.44 \cdot 10^{-10}$ cm/s for D-glucose and D-mannitol, respectively, at 25°C. Papahadjopoulos et al. [21] found a glucose permeability at 36°C of $0.4 \cdot 10^{-10}$ and $0.17 \cdot 10^{-10}$ cm/s for sonicated vesicles made from phosphatidylserine and phosphatidylserine plus cholesterol, respectively. In addition, the roughly 10-fold increase in the non-inhibitable permeability in going from the 4- to 5- and 5- to 6-carbon polyols is approximately what one would expect for diffusion through a lipid membrane since this rate may be determined primarily by the number of hydrogen bonds that must be broken [22]. Thus, the values for the non-inhibitable permeability are quite consistent with the interpretation that

this permeability represents diffusion through the lipid part of the membrane.

However, another interpretation of this non-inhibitable permeability is also consistent. For the pore model shown in Fig. 1, there is the obvious possibility that a solute could fit in the pore even when glucose was present at the binding site. This suggests that the non-inhibitable permeability might actually be associated with the glucose transport mechanism and is not an independent pathway. This possibility is supported by the observation of LaCelle and Passow [10] that the inhibitable and non-inhibitable erythritol permeabilities had an almost identical temperature dependence. One can also calculate a v_p from Eqn. 5 for the non-inhibitable permeability. Since this permeability is measured in the presence of saturating concentrations of glucose, we used the V_{max} for glucose exchange ($3.4 \cdot 10^{14}$ molecules/s per cm^2 [18]) which is about six times larger than the "free carrier exchange" V_{max} that was used in the calculation of the inhibitable v_p. The values of v_p using this V_{max} are shown in Table III (column 5). This v_p represents the volume of distribution in a pore that already contains glucose at the binding site and is easier to interpret than the inhibitable v_p since one does not have to worry about specific affinity for the binding site. We believe that the fact that the values of v_p are in a range that would be predicted for a cell membrane pore is further evidence in support of this second interpretation. However, an argument against this interpretation is the observation that phloretin does not block this non-inhibitable component. If this interpretation is correct it implies that phloretin must be able to block the binding site in the pore without altering the turnover rate, which seems unlikely. A demonstration that the non-inhibitable permeability was definitely associated with the glucose transport system (e.g. by finding a specific inhibitor of glucose transport that also affected the non-inhibitable permeability) would provide strong evidence in favor of the pore model since it would be difficult to explain this association in terms of a carrier mechanism.

Conclusions

A pore that undergoes a conformational change has been proposed as a model of the glucose transport system. The purpose of this paper was to point out that there were some definite predictions that followed from this model and to test these predictions for a series of polyols. In particular, we predicted for the pore model shown in Fig. 1 that: (1) any polyol that was the same size or smaller than glucose should have a finite permeability through the glucose transport system since it could not be prevented from entering the pore volume; (2) This permeability would decrease rapidly as the size of the polyol approached that of glucose, and (3) a "reasonable" volume of distribution in the pore could be determined from Eqn. 5. Although a carrier model cannot be excluded by these results the experimental confirmation of these predictions is at least suggestive evidence in favor of the pore mechanism.

Appendix

(I) Determination of membrane permeability (P) from uptake of radioactive tracers (with no change in cell volume)

The uptake is described by the following basic equation:

$$v_{cw}\frac{dc_{cw}}{dt} = PS[c_e - c_{cw}] \tag{1A}$$

where v_{cw} is the volume of cell water (which is a constant), c_e and c_{cw} are the tracer concentrations in the extracellular and cell water space, respectively, and S is the cell surface area. Since the total amount of tracer is a constant:

$$c_e v_e + c_{cw} v_{cw} = c_e^0 v_e \tag{2A}$$

where v_e is the extracellular volume and c_e^o is the plasma concentration at $t = 0$. Substituting Eqn. 2A into Eqn. 1A:

$$\frac{dc_{cw}}{dt} = P'[c_e^0 - \lambda c_{cw}] \quad \text{where} \quad \lambda = 1 + v_{cw}/v_e;\ P' = PS/v_{cw} \tag{3A}$$

Integrating Eqn. 3A from 0 to t:

$$\ln(1 - \lambda c_{cw}/c_e^0) = -\lambda P' t \tag{4A}$$

In the experiment we actually measured the amount of radidpactivity (A_c) in washed cells from a unit volume of incubation medium:

$$A_c = c_{cw} V_{cw} \tag{5A}$$

where V_{cw} is the volume of cell water per unit volume of the incubation medium. Similarly:

$$A_T = c_e^0 V_e \tag{6A}$$

where A_T is the total radioactivity and V_e is the extracellular volume per unit volume of incubation medium.
Finally:

$$V_{cw}/V_e = KH/(1 - H) \tag{7A}$$

where H is the hematocrit and K is the water fraction of the cell. Substituting Eqns. 5A—7A into Eqn. 4A; the final expression is obtained:

$$\ln(1 - A_c/A_c^{eq}) = -\lambda P' t \tag{8A}$$

where A_c^{eq} is the radioactivity in the cells at equilibrium and is equal to:

$$A_c^{eq} = \frac{KHA_T}{1 - H(1 - K)} \quad \text{and} \quad \lambda = \frac{1 - H(1 - K)}{1 - H} \tag{9A}$$

(II) Determination of permeability (P) from the changes in cell volume

It is not possible to obtain a simple analytic expression for P in these experiments because there are significant changes in the extracellular volume due to the high hematocrit that was used. The procedure adopted was to numerically integrate the equations to obtain the theoretical volume curves for different P values and then find which value of P provided the best fit to the experimental points. The numerical integration procedure was as follows.

Assume that at time t the values of the permeant concentrations in the extracellular space (c_e) and cell water (c_w) and the volume of the extracellular space (V_e) and cell water (V_{cw}) per ml of cell suspension are given. Then in a small time interval τ after t, the amount of permeant per ml of cell suspension (a)

that moves from the extracellular to cellular space is given by:

$$a = P(S/V_c)_0 H_0(c_e - c_{cw}) \tag{10A}$$

where H_o is the hematocrit at $t = 0$ and $(S/V_c)_o$ is the ratio of the surface area to volume of the cell at $t = 0$. It is assumed in Eqn. 10A that the cell volume and the concentrations are constant during the time interval τ. Corresponding to this solute flux there will be a small volume flux (Δ) which can be obtained from the assumption that osmotic equilibrium is maintained:

$$\frac{A_e + V_e c_e - a}{V_e - \Delta} = \frac{A_c + c_{cw} V_{cw} + a}{V_{cw} + \Delta} \tag{11A}$$

where A_e and A_c are the amount of impermeants per ml of cell suspension in the extracellular and cellular space, respectively, and are constant. The assumption of osmotic equilibrium is well satisfied for the slowly permeating solutes used in this study. Eqn. 11A can then be solved for Δ:

$$\Delta = \frac{BV_e - V_{cw}}{1 + B} \quad , \quad B = \frac{A_c + c_{cw} V_{cw} + a}{A_e + c_e V_e - a} \tag{12A}$$

From the value of a and Δ, the values of V and c at time $t + \tau$ can be determined:

$$V'_e = V_e - \Delta \qquad V'_{cw} = V_{cw} + \Delta$$

$$c'_e = (c_e V_e - a)/V'_e; \quad c'_{cw} = (c_{cw} V_{cw} + a)/V'_{cw} \tag{13A}$$

The expression that we wish to compare with the experimental results is the value of the hematocrit at time $t + \tau$ relative to the hematocrit at $t = 0$:

$$H/H_0 = (1 - K) + V'_{cw}/H_0$$

where K is the water fraction of the cell at $t = 0$. Finally, using these new values the entire procedure can be repeated until finally the theoretical curve of H/H_o can be generated for the entire time course.

Since this integration procedure becomes exact as τ approaches zero, its accuracy can be tested by using smaller values of τ. We found by this procedure that if τ was less than 1/50 of the half time then the error was less than 1%. All the theoretical curves that were used to find the best value of P met this criterion.

Acknowledgement

This work was supported in part by a grant from the American National Red Cross Blood Program.

References

1 Geck, P. (1971) Biochim. Biophys. Acta 241, 462–472
2 Regen, D.M. and Tarpley, H.L. (1974) Biochim. Biophys. Acta 339, 218–233
3 Britton, H.G. (1964) J. Physiol. Lond. 170, 1–20
4 Singer, S.J. (1974) Annu. Rev. Biochem. 43, 805–833
5 Jung, C.Y. (1974) J. Biol. Chem. 249, 3568–3573

6 Barnett, J.E.G., Holman, G.D. and Munday, K.A. (1973) Biochem. J. 135, 539—541
7 Bloch, R. (1974) J. Biol. Chem. 249, 3543—3550
8 Bowyer, F. and Widdas, W.F. (1955) J. Physiol. Lond. 128, 7—8p
9 Wieth, J.O. (1971) J. Physiol. Lond. 213, 435—453
10 LaCelle, P. and Passow, H. (1971) J. Membrane Biol. 4, 270—283
11 Ponder, E. (1948) Hemolysis and Related Phenomena, Grune and Stratton, New York
12 Levine, M., Levine, S. and Jones, M.N. (1971) Biochim. Biophys. Acta 225, 291—300
13 Faust, R.G. (1960) J. Cell. Comp. Physiol. 58, 103—121
14 Widdas, N.F. (1954) J. Physiol. Lond. 125, 163—180
15 LeFevre, P.G. and Davies, R.I. (1951) J. Gen. Physiol. 34, 515—524
16 Horton, D., Durette, P.L. and Wander, J.D. (1973) Ann. N.Y. Acad. Sci. U.S. 222, 884—914
17 Lacko, L., Wittke, B. and Kromphardt, H. (1972) Eur. J. Biochem. 25, 447—454
18 Lacko, L., Wittke, B. and Geck, P. (1973) J. Cell. Physiol. 82, 213—218
19 Levitt, D.G. (1974) Biochim. Biophys. Acta 373, 115—131
20 Jung, C.Y. (1971) J. Membrane Biol. 5, 200—214
21 Papahadjopoulos, D., Nir, S. and Ohki, S. (1972) Biochim. Biophys. Acta 266, 561—583
22 Stein, W.D. (1967) The Movement of Molecules Across the Cell Membrane, Academic Press, New York